frontiers in Physics

REVIEW
published: 27 February 2018
doi: 10.3389/fphy.2018.00016

# Laser Surface Texturing of Polymers for Biomedical Applications

*Antonio Riveiro*[1]*, *Anthony L. B. Maçon*[2], *Jesus del Val*[1,3], *Rafael Comesaña*[4] and *Juan Pou*[1,3]

[1] Applied Physics Department, University of Vigo, Vigo, Spain, [2] Department of Materials, Imperial College London, London, United Kingdom, [3] Department of Mechanical Engineering, Columbia University, New York, NY, United States, [4] Materials Engineering, Applied Mechanics and Construction Department, University of Vigo, Vigo, Spain

Polymers are materials widely used in biomedical science because of their biocompatibility, and good mechanical properties (which, in some cases, are similar to those of human tissues); however, these materials are, in general, chemically and biologically inert. Surface characteristics, such as topography (at the macro-, micro, and nano-scale), surface chemistry, surface energy, charge, or wettability are interrelated properties, and they cooperatively influence the biological performance of materials when used for biomedical applications. They regulate the biological response at the implant/tissue interface (e.g., influencing the cell adhesion, cell orientation, cell motility, etc.). Several surface processing techniques have been explored to modulate these properties for biomedical applications. Despite their potentials, these methods have limitations that prevent their applicability. In this regard, laser-based methods, in particular laser surface texturing (LST), can be an interesting alternative. Different works have showed the potentiality of this technique to control the surface properties of biomedical polymers and enhance their biological performance; however, more research is needed to obtain the desired biological response. This work provides a general overview of the basics and applications of LST for the surface modification of polymers currently used in the clinical practice (e.g., PEEK, UHMWPE, PP, etc.). The modification of roughness, wettability, and their impact on the biological response is addressed to offer new insights on the surface modification of biomedical polymers.

**Keywords: laser surface texturing, surface modification, wettability, surface roughness, implants, cell response**

OPEN ACCESS

***Edited by:***
*Narayana Rao Desai, University of Hyderabad, India*

***Reviewed by:***
*Krishna Chaitanya Vishnubhatla, Sri Sathya Sai Institute of Higher Learning, India*
*Khoi Tan Nguyen, Vietnam National University of HCMC, Vietnam*
*Sai Santosh Kumar Raavi, Indian Institute of Technology Hyderabad, India*

***Correspondence:**
*Antonio Riveiro*
*ariveiro@uvigo.es*

***Specialty section:***
*This article was submitted to Optics and Photonics, a section of the journal Frontiers in Physics*

***Received:*** *13 November 2017*
***Accepted:*** *09 February 2018*
***Published:*** *27 February 2018*

***Citation:***
*Riveiro A, Maçon ALB, del Val J, Comesaña R and Pou J (2018) Laser Surface Texturing of Polymers for Biomedical Applications. Front. Phys. 6:16. doi: 10.3389/fphy.2018.00016*

## INTRODUCTION

Polymers are organic materials, formed by linking a large number of repeating units called monomers. These materials are widely used in biomedical applications, e.g., in joint replacement components. Typical polymers used in clinical applications include polyetheretherketone (PEEK), ultra-high-molecular-weight polyethylene (UHMWPE), polypropylene (PP), acrylic bone cements (PMMA), or nylon among others. They exhibit excellent mechanical properties for applications such as knee and hip implants, sutures, orthopedic fixation implants (pins, screws, rods, clips, etc.), dental implants, or stents among others. In addition, they have a reduced density as compared to other biomaterials (such as metals or ceramics), and do not interfere and degrade the biological tissue in contact.

Although these materials are biocompatible, and in some cases, have similar mechanical properties to human tissues, they are, in general, chemically and biologically inert. They show

a minimum interrelation with the surrounding tissues or cells. In consequence, the body usually responds by forming a non-adherent fibrous tissue (through a process called fibrosis) around the surface of the material, and progressively, they are completely encapsulated by such layer. Several works have reported the severe reduction in the mechanical strength of a fibrous encapsulated implant compared with a properly osseointegrated implant [1]. On the other hand, these problems can be worsened by bacterial, viral, or fungal infections occurring around the implant. In this case, the removal of the implant (so-called revision surgery) may be the best alternative, because the fibrous tissue can be impermeable to the medications [2]. One strategy to solve these problems is the application of a bioactive surface coating (e.g., bioactive glass, hydroxyapatite, titanium dioxide, etc.), or to mix these polymers with bioactive materials (e.g., bioactive glass, hydroxyapatite, β-TCP, calcium silicate, etc.) [3–6]. The main problem of coatings is to guarantee a proper adhesion to the polymeric surface. Furthermore, the mixture of polymers with bioactive materials can drastically reduce their mechanical properties. One alternative consists in the application of a surface treatment to enhance the biological properties of the polymers without compromising their mechanical properties. In this way, the fibrosis of implants can be effectively reduced, promoting the tissue integration.

## ROLE OF MATERIAL SURFACE TOPOGRAPHY AND WETTABILITY ON THE BIOCOMPATIBILITY

Biocompatibility is intimately related to the response of cells in contact with the surface of a given material, and in particular with their adhesion [7]. The response of tissues to an implant mainly depends on the physico-chemical properties of its surface. Surface properties such as topography (or texture), surface chemistry, surface energy, or wettability determine the interaction of implants with the biological environment.

The main aim of surface texturing techniques in biomedical applications is the enhancement of the cellular activity in the surface of the implant. In bone remodeling, textured surfaces show a higher surface area for integrating the implant with bone, via osseointegration process. Furthermore, textured surfaces also allow ingrowth of the tissues, and promotes the mechanical stability of implants [8]. Different length scales can be distinguished in an implant surface. Macro-topographies, with surface roughness ranging from millimeters up to microns, can contribute to improve the fixation and long-term mechanical stability of the implant device [9]. Micro-sized topographies, in the range of the microns, affect cell adhesion and proliferation (see **Figure 1**); they have a well-established influence on the improvement of the osseointegration of implants [10]. This kind of features play a key role in the adsorption of proteins. They also affect the cell proliferation, and enhance cell adhesion, and it has been determined their influence on the gene expression for different cell types; therefore, they could be potentially used as a signaling modality for directing differentiation [11].

Another physicochemical property of the implant surface is the interfacial free energy (or in short, surface energy) of the material. This parameter is closely related to the wettability (the preference of a solid to be in contact with one fluid rather than another) of the material. This property is typically evaluated with the water contact angle (WCA), i.e., the angle formed by the interface liquid-vapor with a solid surface (as depicted in **Figure 2**). When a material has a high affinity for water (hydrophilic), i.e., high surface energy, the water spreads on the material and the contact angle is low. In the opposite case (hydrophobic), i.e., low surface energy, water does not spread and forms, at equilibrium, a spherical cap resting on the surface of the material with a large contact angle (see **Figure 2**). It is shown that, more hydrophilic substrates (i.e., with high surface energy, low contact angles) promotes considerably the adhesion and spreading of cells as compared to in hydrophobic materials (i.e., with low surface energy, high contact angles). Air bubbles trapped on the surface of hydrophobic surfaces prevent the protein adsorption to surfaces, and subsequent interaction with cell receptors [10]. This avoids the normal cell adhesion on hydrophobic surfaces (see **Figure 1**). In this sense, Schakenraad et al. [12] demonstrated that the cell spreading is higher on the surface of hydrophilic materials than on hydrophobic (in absence of preadsorbed serum proteins). However, cell adhesion can decrease if the material becomes excessively hydrophilic. This suggest the existence of an optimum range of surface energies [13].

Finally, we should point out that surface topography and wettability of any material are not unrelated properties. Surface roughness can directly affect the wettability of materials and arises as an effective method to control this property. Then, both parameters modulate the biological response.

One of the first attempts to determine the influence of the roughness of any surface on its wettability characteristics was due to Wenzel [14]. He demonstrated the promotion of the intrinsic wettability of a material with the surface roughness. Therefore, if the surface is chemically hydrophobic, it will become even more hydrophobic when surface roughness is added, and vice versa if it is chemically hydrophilic. The results given by Wenzel are based on the assumption that the liquid penetrates into the roughness grooves (see **Figure 3**). In cases where the liquid does not penetrate into the grooves, the Wenzel model does not longer applies. Cassie and Baxter addressed this problem, and assumed that the liquid does not penetrate into the grooves, as depicted in **Figure 3** [15]. The main result of this model is that the presence of air pockets tends to increase the hydrophobicity of the material, independently of its intrinsic wettability. It is generally observed that very rough surfaces are more likely to follow the Cassie-Baxter regime, and low rough surfaces will follow Wenzel's model [16]. Therefore, it can be deduced from this analysis that we can tailor the wettability of the material, and then its biological performance just by changing its surface roughness.

Another standard method to modify the wettability and biological performance of a material is by varying its surface chemistry. Materials with non-polar surfaces, such as polymers, have low surface energy. The modification of the surface chemistry to induce the presence of polar or charged functional

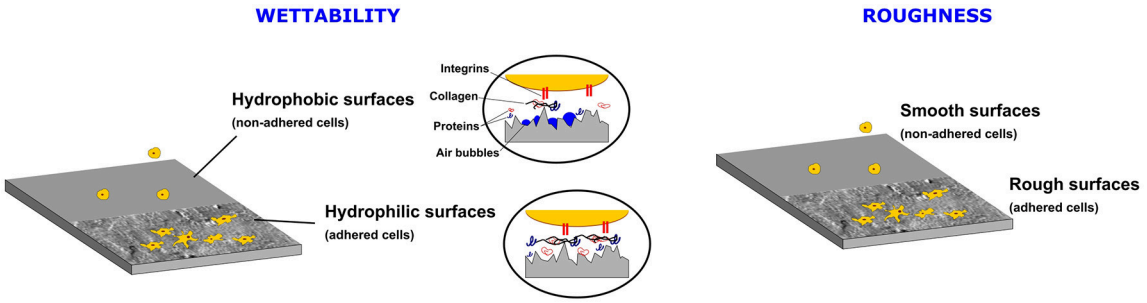


**FIGURE 1 |** Influence of the wettability and surface roughness on the cell adhesion.

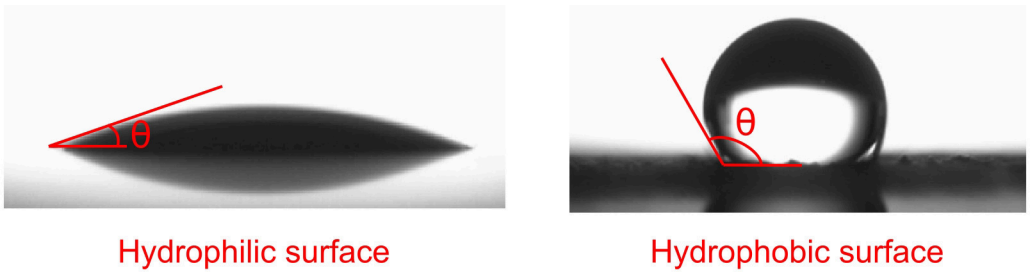


**FIGURE 2 |** Water contact angle for hydrophilic (i.e., with high surface energy), and hydrophobic materials (i.e., with low surface energy).

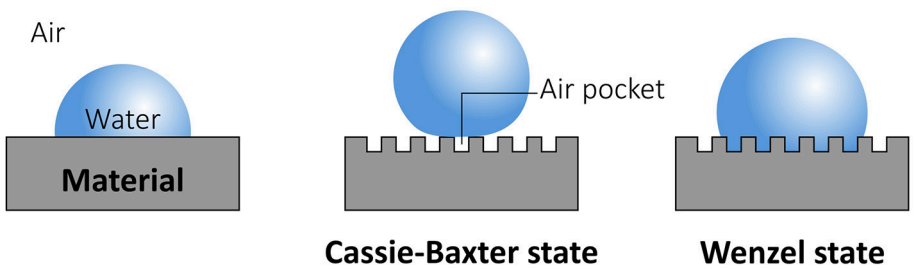


**FIGURE 3 |** Schematic of the influence of the roughness on the wettability. The Cassie–Baxter model proposes that water droplets sitting on rough surfaces form a solid–air–water interface. Air pockets are trapped beneath the droplet. In the Wenzel model, no air pockets form, and the surface is completely wetted by the droplet.

groups is a technique used to increase the wettability of polymers [17].

## BASICS OF LASER SURFACE TEXTURING

### Introduction

Surface modification techniques of polymeric biomaterials for medical implants are performed, in general, in two different ways to promote their biological characteristics. These techniques rely on: (1) deformation, removal or controlled addition of material to the surface to increase the roughness, or (2) by modifying its surface chemistry [18, 19]. Techniques such as photolithography, focused ion beam micromachining, direct writing techniques, or transfer printing, among others, are able to modify polymeric surfaces at the micro- and nanoscale. However, the potentiality of these methods does not cover the full spectrum of requirements needed for the direct treatment of current polymeric biomaterials used in implants [20]. Most of them involve the utilization of toxic chemicals, require multiple steps, sterilization is not guarantee along the treatment (being needed a post-sterilization stage), and production of hierarchical structures is not always possible (see **Table 1**). An alternative technique to these methods, called laser surface texturing (LST; laser texturing, laser structuring, or laser patterning), is based on the direct treatment of polymeric biomaterials with a laser beam. This technique offers a great number of advantages; in particular, the most important is the possible modification of surface roughness and chemistry in one step avoiding the utilization of toxic substances. Laser surface texturing can modify polymeric surfaces at a macro-, micro-, and nano-size scale with a high spatial and temporal resolution [21]. Given the non-contact nature of the process, the contamination of the

**TABLE 1 |** Characteristics of some processing techniques used to produce surface modifications on polymeric biomaterials.

| Technique | Processing rate | Processing steps | Chemical products | Treated area | Cost |
|---|---|---|---|---|---|
| Photolitography | Fast | Several | Yes | Large | High |
| Electron beam litography | Slow | One | No | Small | High |
| Ion beam litography | Slow | One | No | Small | High |
| Atomic force microscopy | Slow | One | No | Small | High |
| Soft lithography | Fast | Several | Yes | Large | Low |
| Chemical vapor deposition | Fast | One | Yes | Large | High |
| Laser texturing | Fast | One | No | Large | Medium |

workpiece is easily avoided; this is a very important advantage for biomedical applications as the sterilization of the implants can be guaranteed. Another advantage is the high processing speed, the easy automation, and the possibility to treat large areas. The simultaneous modification of roughness and chemistry also leads to the simultaneous change of the wettability (or surface energy) of polymers.

The potentiality of this approach to enhance the biological response of biomaterials was largely studied in metals (in particular in titanium alloys) [22–24], and more recently in polymeric biomaterials. Most of the research work done on polymeric biomaterials in this regard only evaluate the biocompatibililty in terms of the change in roughness and wettability with the laser treatment. More recently, some research works (using *in vivo* and *in vitro* tests) have been performed to elucidate this enhancement in the biological response of the laser-treated polymeric biomaterials; however, more studies are still needed to transfer this technique into the current clinical practice. With this work, we intend to complement reviews on laser patterning, mainly concentrated on laser ablation mechanisms (e.g., [21, 25–27]), and to provide the reader with a critical understanding on the next steps to advance in this field.

## Process Fundamentals

LST is one of the simplest techniques to modify both surface topography and chemistry [28]. In this case, a focused laser beam is directed onto the surface of some material; then, the laser radiation is absorbed by the topmost layer (**Figure 4**). The optical energy provided by the laser beam induces the heating of the material, reaching the melting, or even the vaporization temperatures. This way a selective material removal is achieved, and the surface topography is modified. On the other hand, if the photons of the laser beam are sufficiently energetic, e.g., using UV-lasers, they are able to break chemical bonds, and then modifying the surface chemistry of the material. Therefore, thermal and/or photochemical processes can modify the surface of polymers:

- Thermal processes: the temperature of the material is increased by the thermalization of the optical energy in the surface of the material. This phenomenon leads to diverse induced phenomena, including melting or vaporization [29]. In general, these phenomena induce the modification of the surface roughness.
- Photochemical processes: the energy of photons emitted by the laser source is so high that directly breaks the molecules of the treated surface. This mechanism is the main responsible for the chemical modification of surfaces. In this case, due to the necessity of high energy photons, ultraviolet (UV) lasers are the most commonly employed ones [30].
- Photophysical processes: in this case, thermal and photochemical process jointly influence on the process [31]. In this case, both surface roughness, and chemistry can be simultaneously modified.

LST can be performed by the creation of regular or irregular patterns of bumps, dimples, and (linear or non-linear) grooves as depicted in **Figure 4** [28]. The resulting surface topography and chemistry depends on the preponderance of thermal, or non-thermal processes. If the surface of the material is melted, bumps or dimples can be formed due to the formation of projections, depressions or due to the foaming of the material. The increased absorption of laser radiation can produce the vaporization of the material. In this case, removal of material is mainly produced by the vaporization or thermal decomposition, but some melting or thermal degradation can also occur. Non-thermal processing associated to the utilization of ultrafast lasers can also produce dimples and grooves, but avoiding undesirable thermal effects (e.g., generation of a heat affected zone). In this case, the direct breaking of molecular or atomic bonds takes place, rather than simply heating. Therefore, this is a clean process, leaving no recast material and eliminating the need of post-processing steps [31].

Patterns in biomedical polymers can be produced in the UV–IR spectral range, using continuous-wave (CW) or pulsed laser radiation [32, 33]. Influence of the processing parameters, their effects, and theoretical modeling is complex. It depends on multiple parameters associated to the nature of the polymer and the specific working approach used to produce the surface topography (e.g., photo-thermal or photo-chemical ablation of the material, laser swelling or bumping, laser grooving, etc.). These analyses are beyond the scope of this work. We refer the interested reader to the specialized works for further information (e.g., [21, 34–41]).

Absorption characteristics of polymers depends on their structure, but this behavior is influenced by the presence of fillers or additives. UV radiation is preferred for LST as seen in **Table 2**, but other laser wavelengths are also used. IR radiation tends to produce the thermal ablation or melting of polymers, while the treatment with UV radiation is able to ionize and decompose polymers without substantial melting. This laser radiation can also modify the surface chemistry of polymers. In this case, the polar component of the surface energy can be considerably increased, and the wettability can be promoted (see e.g., [42]).

Compared to pulsed laser radiation, CW operation mode produces patterns with low quality, and high thermal affectation

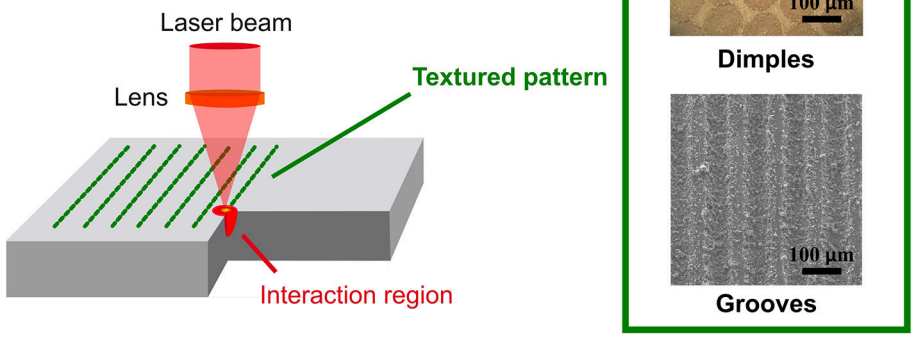


**FIGURE 4 |** Schematic of the principle of operation of laser surface texturing (LST).

around the laser-treated area. Then, this processing mode is scarcely used (see **Table 2**). On the contrary, the reduction in the pulse length produces high precision patterns. In the case of processing with ultrashort (picosecond or femtosecond) laser pulses, the heat diffusion into the polymer is avoided, and the thermal damage close to the radiated area is negligible [76]. Therefore, debris formation can be avoided. This is interesting as any potential source of debris in implants must be avoided. Released implant debris induces inflammation and osteolysis around the implanted area, and compromises the performance of implants [77]. Another relevant feature about using ultrashort pulses is the high intensities produced in the irradiated area. These are able to produce nonlinear optical phenomena, such as multiphoton absorption. Then, molecular bond breaking or even ionization can be reached even though the wavelength of the laser radiation is theoretically long (i.e., low photon energies) [78].

Other laser and non-laser related processing parameters are listed in **Table 2**. These also depend on the nature of the polymer. In general, focused laser beams onto the surface of the samples are used, with spot diameters ranging from several to hundred (even thousands) of microns. LST experiments are predominately performed in air atmosphere (see **Table 2**); however, the influence of the processing atmosphere should not be neglected as this affects the surface chemistry and the wettability of the laser-treated surfaces. Pfleging et al. [71] observed a marked increase in the wettability of PMMA using $O_2$ (instead of He) as processing gas during laser processing of PMMA. XPS measurements showed the oxidation of the PMMA surfaces during the processing with $O_2$. However, the influence of this processing parameter on the biological performance of laser textured samples has not yet been evaluated, and this evaluation should be addressed in future studies.

## Components of a Laser Texturing System

There are two main methods for laser texturing: (1) using a stationary laser beam, or (2) providing a relative movement between the laser beam and the surface of the workpiece.

The first approach requires the utilization of a mask with the desired pattern. Then, only the portion of light that passes through the mask is imaged by a lens to produce a pattern on the surface of the workpiece (see **Figure 5**). In this case, a short laser pulse (required to obtain high peak powers) is used to produce the pattern; then, pulsed lasers (such as excimer, femtosecond, or TEA $CO_2$ lasers) are utilized. This approach is not commonly used (see **Table 2**) as it is less flexible. Production of a mask is a time-consuming process, and the modification of the textured pattern necessarily requires the production of new masks. Furthermore, some small structures can be formed around the textured pattern due to the laser beam diffraction at the mask geometry [71]. Other approach also using a stationary laser beam is the laser interference patterning, or direct laser interference patterning (DLIP) [70]. This technique involves the interference of two or more laser beams to obtain a periodic variation of light intensity on the irradiated area. This approach can produce very fine details, and even the production of hierarchical structures with two different length scales. This posibility can be very attractive to promote osteoconductive and osteoinductive properties because the cell response (morphology, adhesion, proliferation, etc.) depends on the micro- and nano-topography [79]. However, this technique is less flexible than using a mask: (1) the modification of the pattern is not simple (the production of a defined interference pattern requires a complex and time consuming procedure to superimpose the laser beams with high accuracy), and (2) the system is more expensive [80].

In the second case, the relative motion of the laser beam with regard to the workpiece produces the pattern. This can be done moving the beam or the workpiece. Two common ways

**TABLE 2 |** Summary of processing parameters and research aims of selected works found in the literature on LST of clinically relevant polymers.

| Material | Form/ thickness | Laser | λ (nm) | Power (W) | Spot diameter (μm) | Fluence (J/cm$^2$) | Focal length (mm) | CW/P | Freq. (Hz) | Pulse duration | Pulse number | Texturing approach & morphology | Scanning speed (mm/s) | Atmosphere | Application | Ref. |
|---|---|---|---|---|---|---|---|---|---|---|---|---|---|---|---|---|
| PEEK | Film 250 μm | ArF excimer | 193 | – | – | 5-80x10$^{-3}$ | – | P | 10 | 20 ns | 1–2,000 | Stationary beam/Conical structures | – | Ar, Air, $O_2$ | Influence on adhesive bonding properties | [43] |
| PEEK | Plate 8 mm | Nd:$YVO_4$ | 1,064 | 5–39 | 100–1,000 | – | 211 | P | 15,200–50,000 | ∼ns | – | Galvanometric scanning system/Parallel grooves | 200–5,000 | Air | Biomedical (Increment of roughness and wettability) | [44] |
| | | Nd:$YVO_4$ | 532 | 5–39 | 100–1,000 | – | 365 | P | 15,200–50,000 | ∼ns | – | Idem | 200–5,000 | Air | | |
| | | Nd:$YVO_4$ | 355 | 5–39 | 100–1,000 | – | 235 | P | 15,200–50,000 | ∼ns | – | Idem | 200–5,000 | Air | | |
| PEEK | – | Nd:YAG | 355 | – | 450 | 0.75 | – | P | – | 38 ns | 4–12 | Interference patterning/Line structures | – | – | Biomedical (influence on cell growth) | [45] |
| PEEK | – | ArF excimer | 193 | – | – | 3.5 | – | P | – | 20–25 ns | 10 | Stationary beam + Mask/Parallel grooves | – | – | Biomedical (Influence on pre-osteoblastic cell response) | [46] |
| PEEK | Membranes 240 μm | $CO_2$ | 10,600 | 1 | – | – | 100 | Quasi-CW | 5,000 | ∼ms | – | Galvanometric scanning system/ Parallel grooves | – | Air | Biomedical (Influence on osteoblast response) | [47] |
| PEEK | Plate 3.92 mm | Q-Switched Nd:YAG | 1,064 | – | 600–2,500 | 0.01–0.1 | – | P | 10 | 10 ns | – | XY Table/Dimples | 12 | Air | Influence on adhesive bonding properties | [48] |
| PEEK | Foil 50 μm | KrF Excimer | 248 | – | – | 0.004–0.03 | – | P | 10 | 20–40 ns | 6,000 | XY Table/Ripple & dot patterns | – | – | Biomedical (Influence on wettability, roughness, chemistry and cell adhesion) | [49] |
| PEEK | Sheet 2 mm | Ti:sapphire | 800 | 0.02 | – | – | – | P | 1,000 | – | – | Parallel grooves | 1 | Air | Biomedical (Influence on osteogenic response) | [50] |
| PEEK+ Nano-$SiO_2$ | Sheet 2 mm | Ti:sapphire | 800 | 0.02 | – | – | – | P | 1,000 | – | – | Parallel grooves | 1 | Air | | [50] |
| UHMWPE | Sheet 1 mm | Q-Switched Nd:YAG | 1,064 | – | – | 0.6 | – | P | 0.5 | 9 ns | 10–50 | Stationary beam/Rough surface | – | Air | Influence on wettability | [51] |
| | | Q-Switched Nd:YAG | 532 | – | – | 0.6 | – | P | 0.5 | 9 ns | 10–50 | Idem | – | Air | | |
| | | KrF excimer | 248 | – | – | 0.6 | – | P | 0.5 | 23 ns | 10–50 | Idem | – | Air | | |
| | | XeCl excimer | 308 | – | – | 0.6 | – | P | 0.5 | 20 ns | 10–50 | Idem | – | Air | | |
| UHMWPE | Sheet 1 mm | Nd:YAG | 532 | – | 6,000 | 0.5 | No lens | P | 10 | 3 ns | 0 | Stationary beam/ Rough surface | – | Air | Influence on roughness | [52] |
| UHMWPE | – | $CO_2$ | 10,600 | – | – | <2.5 | – | P | – | 30 ns | 20–50 | Stationary beam/Rough surface | – | Air | Influence on roughness, wettability and chemistry | [53] |
| | – | KrF excimer | 248 | – | – | 0.3 | – | P | – | 23 ns | 20–50 | Stationary beam/Rough surface | – | Air | | |
| UHMWPE | Disk 3 mm | Yb:KYW femtosecond | 1,027 | – | 8 | 2–14 | – | P | 1,000 | 450 fs | – | XYZ Table/ Rough surface | 1–2 | Air | Influence on surface topography and chemistry | [54] |
| UHMWPE | Plate 8 mm | Nd:$YVO_4$ | 1,064 | 0.8–6 | 70 | <8.3 | 211 | P | 15,200–50,000 | ∼ns | – | Galvanometric scanning system/Parallel grooves | 200–5,000 | Air | Biomedical (Influence on roughness and wettability) | [55] |
| | | Nd:$YVO_4$ | 532 | 1.5-6.5 | 60 | <11.4 | 365 | P | 15,200–50,000 | ∼ns | – | Idem | 200–5,000 | Air | | |
| | | Nd:$YVO_4$ | 355 | 0.3–1.4 | 25 | <11.4 | 235 | P | 15,200–50,000 | ∼ns | – | Idem | 200–5,000 | Air | | |
| PP | – | ArF excimer | 193 | – | – | 0.0125 | – | P | – | – | 0–10,000 | Stationary beam/Surface | – | Tap water | Influence on bonding characteristics | [56] |
| PP | – | Ti: sapphire | 800 | – | 60 | 0.4–3.2 | – | P | 5,000 | 130 fs | 1-50 | XY Table /Craters | – | Air | Influence on surface properties | [57] |
| PP | – | Nd:YAG | 1,064 | – | 7,000 | 5 | – | P | 10 | 2-8 ns | – | – | – | Air,$O_2$,$N_2$ | Influence on bonding characteristics | [58] |
| | | Nd:YAG | 532 | – | – | 2.5 | – | P | | 1–2 ns | – | – | – | Air,$O_2$,$N_2$ | | |
| | | Nd:YAG | 266 | – | – | 0.45 | – | P | | 3–4 ns | – | – | – | Air,$O_2$,$N_2$ | | |
| PP | Sheet 5 mm | KrF excimer | 248 | – | – | 5 | – | P | 1 | – | – | Stationary beam/Rough surface | – | Air | Biomedical (Influence on roughness, wettability, cell proliferation) | [59] |

*(Continued)*

**TABLE 2** | Continued

| Material | Form/ thickness | Laser | λ (nm) | Power (W) | Spot diameter (μm) | Fluence (J/cm$^2$) | Focal length (mm) | CW/P | Freq. (Hz) | Pulse duration | Pulse number | Texturing approach & morphology | Scanning speed (mm/s) | Atmosphere | Application | Ref. |
|---|---|---|---|---|---|---|---|---|---|---|---|---|---|---|---|---|
| PE | Film 300 μm | Nd:YAG | 532 | – | 1,100 | 1.4–6.3 | 300 | P | 1 | 10 ns | 1–300 | Stationary beam /Dimple | – | – | – | [60] |
| Low-density PE | Film 50 μm | TEA $CO_2$ | 9,580 | – | – | 1.2 | – | P | 0.5 | – | 1–3 | Stationary beam/Rough surface | – | Air | Influence on surface properties | [61] |
| PE | Sheet 2 mm | Ti:sapphire | 790 | – | 1.5 | <0.11 | 150 | P | – | 130 fs | – | Stationary beam + Mask/Dimple | – | Air | Influence on surface properties | [62] |
| | | Ti:sapphire (second harmonic) | 395 | – | 1.5 | <0.08 | 150 | P | – | 130 fs | – | Idem | – | Air | | |
| | | | 395 + 790 | – | 1.5 | <0.08 | 150 | P | – | 130 fs | – | Idem | – | Air | | |
| | | ArF excimer | 193 | – | – | <0.08 | – | P | 10 | 23 ns | – | Idem | – | Air | | |
| | | Molecular fluorine ($F_2$) | 157 | – | – | <0.02 | – | P | 10 | 20 ns | – | Idem | – | Air | | |
| PE | Sheet 2 mm | Nd:YAG | 1,064 | – | – | – | – | P | 500 | – | – | – | 1 | – | Biomedical (Influence on biological response) | [63] |
| Bisphenol-A PC | Thin film 3 μm | KrF excimer | 248 | – | – | <0.35 | – | P | 1 | 30 ns | 5 | Stationary beam/Rough surface | – | Air | Biomedical (Influence on roughness) | [64] |
| PC | Film | ArF excimer | 193 | – | – | 0.01–0.02 | – | P | 10 | 20 ns | 1–1,000 | X–Y Table | – | Air, Ar | Biomedical (Influence on chemistry, wettability) | [65] |
| | | | 248 | – | – | 0.01-0.03 | – | P | 10 | 30 ns | 1–1,000 | Idem | – | Air, Ar | | |
| PC | Film 1 mm | Nd:YAG | 1,064 | – | 0.8-3 | 0.42-19.9 | – | P | 1 | 10 ns | 1-5 | Rotating table/Craters | - | Air | Biomedical (Influence on fibroblast response) | [66] |
| | | | 355 | – | 3 | 0.42 | – | P | 1 | 10 ns | 1-5 | Idem | – | Air | | |
| Nylon 6,6 | Sheet 5 mm | $CO_2$ | 10,600 | 7 | 95 | – | 250 | CW | – | – | – | Galvanometric scanning system/ Parallel grooves | 600 | Air | Biomedical (Influence on fibroblast response) | [67] |
| Nylon 6,6 | Film 1 mm | $CO_2$ | 10,600 | 7–10 | – | – | – | – | – | – | – | Galvanometric scanning system/Parallel grooves | 600 | Air | Biomedical (Influence on roughness, wettability, cell response) | [68] |
| PI | Film 3 μm | Nd:YAG | 355 | – | – | 0.1-1 | – | P | 10 | 10 ns | – | Interference patterning/Line structures | – | Air | Biomedical (Influence on cell response) | [69] |
| PI | Film >2 mm | Nd:YAG | 355 | – | – | 0.1-3 | – | – | 10 | 10 ns | – | Interference patterning/ Dot & line structures | – | Air | Influence on surface topography | [70] |
| | | Nd:YAG | 266 | – | – | 0.1–3 | – | – | 10 | 10 ns | – | Idem | – | Air | Influence on surface topography | |
| PMMA | – | ArF excimer | 193 | – | – | 0.02–0.09 | – | P | – | 20 ns | 1-1,200 | Grooves | – | Air, $O_2$, He | Biomedical (Influence on wettability, chemistry, cell adhesion) | [71] |
| PMMA | Sheet 3 mm | Ti:sapphire | 800 | – | 20.4 | 0.85–50 | 100 | P | 1,000 | 150 fs | 20 | XY Table/Parallel grooves | 1 | Air | Influence on surface properties | [72] |
| PMMA | Film 1 mm | Ti:sapphire | 800 | – | 1.5–2.4 | – | – | P | 1,000 | 100 fs | - | XYZ Table/Craters | – | Air | Influence on surface topography | [73] |
| PMMA | Film 1 mm | Ti:sapphire | 775 | – | 29 | 0.1-50 | 100 | P | 1,000 | ~fs | – | Parallel grooves | 2 | | Microfluidics | [74] |
| PMMA | Film 1 mm | Ti:sapphire | 800 | – | 1.5-2.4 | – | – | P | 1,000 | 100 fs | – | XYZ Table/Craters | 1 | Air | Microfluidics | [75] |

*CW, Continuous wave; P, Pulsed.*

of doing this are: the utilization of a Cartesian system to move the laser beam (see **Figure 6A**), or steering the beam over the workpiece via two galvanometer mirrors (see **Figure 6B**). The last approach is more commonly selected due to the higher versatility, and throughput. In both systems, CW or pulsed lasers can be used.

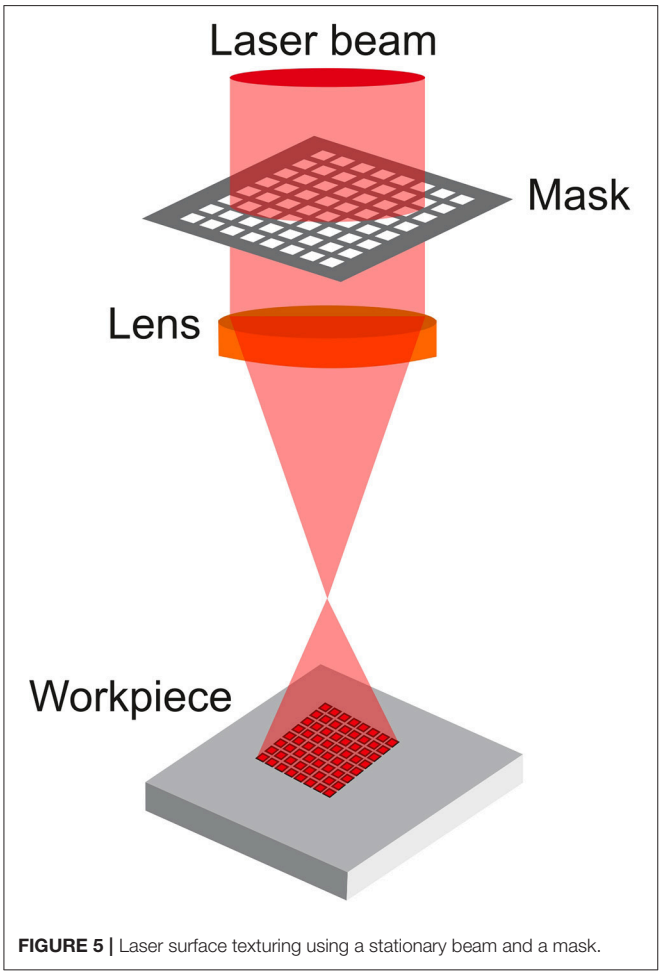


**FIGURE 5 |** Laser surface texturing using a stationary beam and a mask.

As seen in **Table 2**, different laser sources are used for LST. UV laser radiation is generated by excimer (e.g., ArF or KrF), or solid-state lasers (e.g., frequency tripled); however, the better beam quality of solid state lasers, and the non-utilization of toxic gases (in contrast with excimer lasers) make solid-state lasers more attractive for LST. Nd:YAG or Nd:$YVO_4$ lasers emitting ns laser pulsed in the NIR range are also used. Ti:sapphire lasers, emitting 800 nm laser radiation, were used to produce fine patterns. Far-IR laser radiation from $CO_2$ lasers is barely used.

## LASER SURFACE TEXTURING OF BIOMEDICAL POLYMERS

Multiple polymeric biomaterials have been studied for tissue engineering [81–83]; however, only few of them are really used in the current clinical practice. Therefore, we will review the main research works on LST of those currently used for medical applications, especially on those used in bone tissue engineering [84].

### Poly(etheretherketone) (PEEK)

Polyetheretherketone (PEEK) is an engineering thermoplastic that exhibits a rigid semicrystalline structure. It shows excellent mechanical properties (in some cases, even similar to cortical bone), and high chemical resistant [85]. In addition, PEEK exhibits sterilization capacity [86]. These properties turn it into an ideal material to be used in biomedical applications. This polymer is mainly used as structural material in orthopedic applications (e.g., in joint replacement, cage implants, bone screws, and pins, etc.); however, it is biologically inert due to its large chemical stability, and low wettability (see **Table 3**). This leads to poor bone-implant interactions.

First studies on LST of PEEK were performed by Laurens et al. using excimer lasers [43]. It was demonstrated the ability of ArF laser ($\lambda = 193$ nm and pulse duration $= 20$ ns) to modify PEEK surfaces below the ablation threshold. The chemical modification after laser treatment depended on the assist gas used in the process (i.e., a neutral or an oxidizing atmosphere). Under neutral conditions, loss of polymer aromaticity and scission of carbonyl groups took place. In the presence of

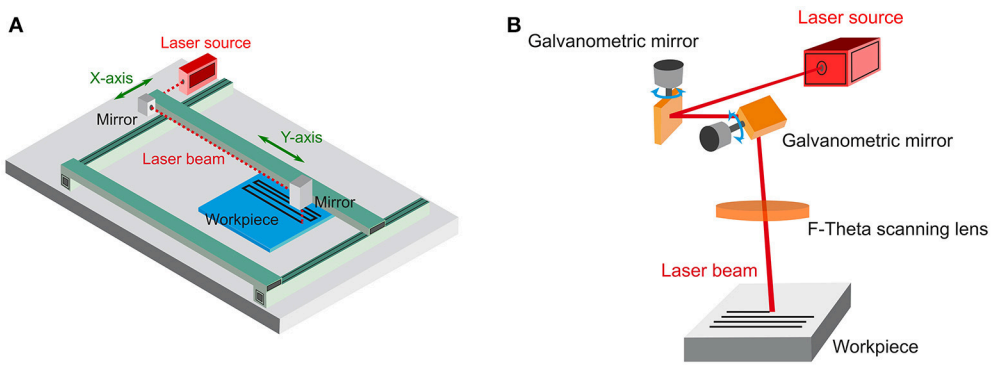


**FIGURE 6 |** Laser surface texturing by imposing a relative movement between the laser beam and the workpiece using **(A)** a cartesian, or **(B)** a scanning system.

**TABLE 3 |** Surface roughness and contact angle of pristine polymeric biomaterials, and after laser surface texturing experiments.

| Material | Laser/wavelength (nm) | $R_a$ (μm) | θ(°) | $R_a$ (μm) | θ(°) | References |
|---|---|---|---|---|---|---|
| | | Base material | | Laser treated surface | | |
| PEEK | KrF excimer/248 | $1.4{\cdot}10^{-3}$ | 69.4 | $17{\cdot}10^{-3}$ | 50 | [49] |
| PEEK | Ti:Sapphire/800 | 0.3193 | 79.3 | 0.6245 | 54.8 | [50] |
| UHMWPE | KrF excimer/248 | 0.075 | 94 | 0.6 | 86 | [53] |
| UHMWPE | Nd:$YVO_4$/1,064 | 2.3 ± 0.4 | 82 ± 5 | 2.3 ± 0.7 | 75.2 ± 10 | [55] |
| UHMWPE | Nd:YAG/1,064 | – | 94 | – | 90 | [51] |
| Nylon 6,6 | $CO_2$/10,600 | 0.29 | 66.49 ± 0.32 | 0.83 | 57.5 ± 2.50 | [68] |
| PP | KrF excimer/248 | 0.0163 | 99 | 0.02023 | 76 | [59] |
| PP | Nd:$YVO_4$/1,064 | 0.057 | 86.1 ± 2.0 | 4.04 | 89.9 ± 13 | [87] |

environmental oxygen, the high energetic incoming photons increased the C-O/C, and carboxylic functions. Furthermore, the polar component of the work of adhesion increased after laser treatment. Similar results were also observed by Michaljaničová et al. [49] during the treatment of PEEK surfaces with UV radiation ($\lambda = 248$ nm). In this case, an increase of the wettability is observed (see **Table 3**). This was attributed to the increase in roughness, and oxygen containing groups formed on the treated surfaces.

More recently, other laser wavelengths were studied with the aim to evaluate their effect on the surface modification of PEEK [44, 47, 48]. So far, surface functionalization of PEEK by means of LST has been successfully achieved using laser wavelengths ranging from UV (355 nm) to middle infrared (MIR) (10.6 μm).

Riveiro et al. compared the effect of the three ns laser irradiation wavelengths (355, 532, and 1,064 nm) on the roughness, and contact angle of PEEK substrates, properties directly related to the cell viability on implants [44]. In order to enhance its adhesion properties, an increase on the wettability was sought. PEEK was observed to respond very differently as a function of the laser radiation (see **Figure 7**). The 1,064 m laser radiation burned the surface, while the 532 nm laser radiation was able to ablate the material. Using this laser wavelength, grooves with a mean width of 100 μm were machined. The 355 nm laser radiation only produced a slight surface melting; however, this laser radiation was identified as the most suitable for biomedical purposes because induced the formation of some polar groups [carboxyl (O-C=O) and peroxide (O-O)] on the surface of the PEEK samples. They produced a marked reduction in the WCA of PEEK after treatment. This fact can be potentially beneficial to promote cell adhesion onto laser treated PEEK. A similar effect was observed by exposing PEEK to Q-switched Nd:YAG laser radiation ($\lambda = 1{,}064$ nm) [48]. In this case, the surface energy was increased (from 44.9 to 78.5 $mJ/m^2$), along with the wettability, after the laser treatment. Chemical analyses suggested that an increase in hydroxyl and carboxylic groups, along with a decrease on the original carbonyl groups, took place after laser treatment. It was showed the formation of functional polar groups on laser-treated PEEK surfaces. These findings confirmed the NIR lasers as a viable option to promote the functionalization of PEEK surfaces by LST.

These studies only assessed the biocompatibility of laser treated surfaces in terms of the wettability; however, this does not guarantee the biocompatibility of the surfaces, and biological tests (*in vitro* and also *in vivo* tests) are required.

The enhancement of biocompatibility of the laser textured PEEK surfaces attributed to the formation of polar groups was confirmed by Zheng et al. [47]. *In vitro* tests, along with topographical, and chemical analyses on PEEK surfaces modified by a combination of $CO_2$ laser ($\lambda = 10{,}600$ nm) and plasma treatments, were conducted. MC3T3-E1 pre-osteoblast were the cells employed in this study. Cell adhesion and proliferation were increased after laser treatment, in conjunction with an increase in the formation of carboxylic groups on the surface. Therefore, it was established the direct relationship between the roughness and the formation of polar groups with the increased biocompatibility of laser-treated PEEK surfaces [47]. Guo et al. [50] focused their attention to the influence of the roughness on the biological activity and osteogenic efficiency of laser-treated surfaces. Femtosecond laser irradiation was used to modify the surface of PEEK implants (with and without the reinforcement of nano-$SiO_2$ particles). *In vivo* animal tests were performed on rabbits, and demonstrated a superior bonding strength of the bone/implant interface for treated implants. A similar result was found by Briski et al. [88] during implantation of laser textured PEEK cages for fusion in a sheep model. Enhanced fusion and higher deposition of mineralized matrix was observed after 6 months of implantation.

Cordero et al. [46] studied the influence of micro-grooves patterns on the cell alignment of MC3T3-E1 pre-osteoblasts. Patterns were produced with UV light (from an ArF laser) using a mask projection unit. The increased cell growth along preferential directions is proposed to act as a bridge for the bone regeneration in disrupted areas. *In vitro* results, showed a better cell alignment for patterns formed with lines separated distances below 50 μm. Bremus-Koebberling et al. [45] followed a similar approach, but using nano-grooves. They evaluated the influence of linear-like nanopatterns produced by laser interference patterning ($\lambda = 355$ nm, pulse duration = 38 ns) on the cell alignment using B35 neuronal cells. In this case, the main aim was their utilization for neuronal repair applications. It was demonstrated that not only the pattern periodicity (i.e.,

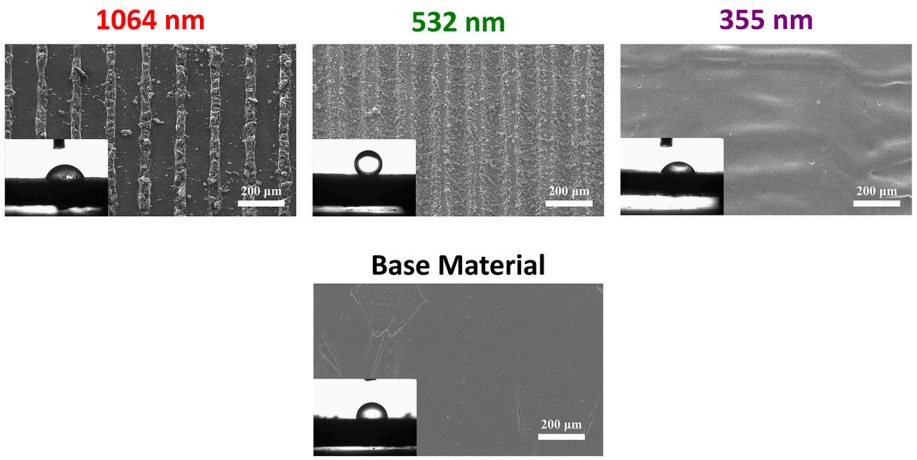


**FIGURE 7 |** SEM images of the laser treated PEEK surfaces under 1,064, 532, 355 nm laser wavelengths, and for the base material. Insets: optical images of water drops deposited onto untreated and laser treated PEEK surfaces (untreated PEEK: contact angle 92.4°, 1,064 nm laser radiation: contact angle 59.5°, 532 nm laser radiation: contact angle 131.0°, 355 nm laser radiation: contact angle 52.5°). Adapted from [44] with permission from Elsevier.

the width of the nano-grooves), but also the groove depth (or more precisely, the aspect ratio) influences the cell alignment. These results demonstrate that nano-topography is relevant for the control of the cellular response. They also open the door for the application of laser-textured patterns not only for bone tissue engineering, but also for other biomedical applications.

## Ultra-High-Molecular-Weight Polyethylene (UHMWPE)

Ultra-high-molecular-weight polyethylene (UHMWPE) is a thermoplastic synthetized from monomers of ethylene (-$(CH_2)_n$-), used as a bearing material in joint replacement implants for decades. It is commonly used in biomedical applications such as in patella or hip prostheses [51, 55]. This is principally due to its high wear and impact resistance, chemical stability, and non-toxicity in contact with corporal fluids. However, the large chemical stability, and low wettability (see **Table 3**) make this material also bioinert.

Laser surface modification on UHMWPE has been successfully demonstrated by means of fs, ps, and ns laser sources. Laser treatments produces the increment of the roughness and wettability (see **Table 3**).

Pulsed Yb:KYW fs laser ($\lambda = 1{,}027$ nm, and pulse duration = 450 fs) was used to create size-controlled craters on UHMWPE surfaces. The maximum ablation efficiency was obtained using laser pulse energies above 6 µJ. The surface chemistry of UHMWPE was found to remain virtually unaltered after laser interaction [54]. However, by subjecting this thermoplastic to ps laser surface radiation (from the iodine PALS -Prague Asterix Laser System- laser), different results were revealed [89]. In this case, 438 nm laser pulses, with a high energy (up to 240 J) and a short pulse length (400 ps) were used. The chemical analyses of the irradiated surface confirmed substantial changes in the ablated crater composition when compared to the pristine UHMWPE substrate. The results from the mass quadrupole spectrometer (MQS) showed that C-H, and C-C chemical bonds were broken given the high deposited energy during the ablation process. Also, Raman spectroscopy and infrared absorption analyses demonstrated the enrichment in carbon content of the laser affected areas.

Lorusso et al. [51] evaluated the influence of the laser treatment on the wettability using IR ($\lambda = 1{,}064$ nm), visible ($\lambda = 532$ nm), and UV laser radiation ($\lambda = 308$ and 248 nm). They found a decrease of the WCA with the number of pulses (irrespectively of the laser wavelength). This reduction is more marked for surfaces treated with UV laser radiation. These results are explained in terms of the interaction mechanisms with the substrate. IR and visible laser pulses induces photothermal effects, while UV radiation is able to produce photochemical effects. It is postulated that they modify the surface chemistry. Velardi et al. [53] also found using 248 nm UV laser radiation (and similar processing parameters) that this laser wavelength produces the formation of oxidized groups (such as hydroxyl and carbonyl). A similar decrease in the WCA, and the increment of the average roughness with the number of pulses was also observed. Then, the increment of the wettability is mainly ascribed to the modification of the surface chemistry.

Riveiro et al. studied the modification of UHMWPE with several laser wavelengths (1,064, 532, and 355 nm) [55]. In this work, a carbon coating was applied on the surface of the UHMWPE samples to reduce the large transparency exhibited by this material to these laser wavelengths. Raman spectroscopy revealed that UHMWPE undergoes minor chemical modifications after the laser treatments. The visible and UV laser wavelengths were found the most suitable to tailor the topography, and wettability. In both cases, the average roughness was closer to $R_a = 1$ µm, and the WCA was reduced compared to the pristine surface (**Figure 8**). Nevertheless, due to the melting of the surface after the laser treatment, some carbon particles were trapped during the process (**Figure 8**);

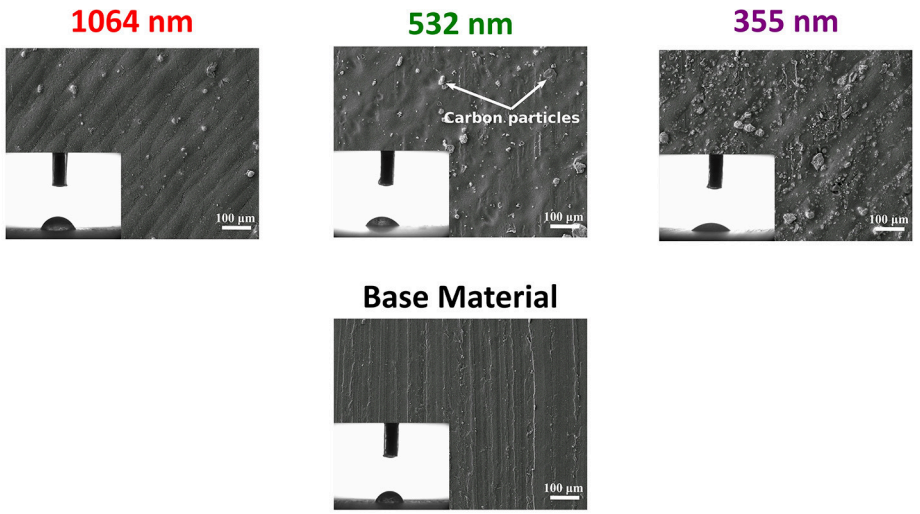


**FIGURE 8 |** SEM images of the laser treated UHMWPE surfaces under 1,064, 532, 355 nm laser wavelengths, and for the base material. Insets: optical images of water drops deposited onto untreated and laser treated UHMWPE surfaces (untreated UHMWPE: contact angle 71°, 1,064 nm laser radiation: contact angle 71.7°, 532 nm laser radiation: contact angle 56.2°, 355 nm laser radiation: contact angle 54.8°). Adapted from [55] with permission from Elsevier.

however, they are not considered a risk because it is reported that carbon particles do not elicit a toxic response on tissues or heavy inflammatory reactions. A large amount of microcracks in the surface of the 1,064 nm laser treated area was observed. Their formation was attributed to the larger thermal effects (which causes thermal stresses) produced by this radiation. Although cell viability tests were not performed in this study, the values of roughness obtained through the treatment, and the formation of polar carbon clusters suggested to be beneficial for biological compatibility purposes [90, 91].

## Polypropylene (PP)

Polypropylene is a biocompatible thermoplastic polymer showing good biostability, good thermal stability, and appropriate mechanical properties [92]; however, PP exhibits low surface energy (see **Table 3**), which hinders its systematic use for tissue replacement. Several techniques were studied to increase the low interface energy, such as the deposition of coatings [93], plasma treatment [94, 95], graft polymerization [96], and injection molding [97]. Nevertheless, a precise control in the process, and subsequent surface modification remained as a major challenge.

Belaud et al. created micro- and nano-sized structures on PP surfaces using fs laser pulses [57, 98]. A infrared laser beam (Ti:Sapphire laser, $\lambda = 800$ nm), with a short pulse duration (130 fs in pulse length), was used in this study. The ablation of the surface was identified as the main physical mechanism leading to the surface modification of PP; however, the surface modification or ablation of PP was seen enhanced with the coating of PP with silver 2–3 µm thick.

A further insight into the effect of laser textured PP surfaces on their potential applicability in biological applications was provided by Riveiro et al. [87]. It was demonstrated the ability of ns lasers (pulse duration $< 100$ ns) to successfully texture PP surfaces. The effect of treatment under 1,064, 532, and 355 nm laser wavelengths on the surface features of PP was evaluated. A layer of carbon black was used to increase the original absorption features of this thermoplastic given its high transmittance for wavelengths ranging between 400 and 1,600 nm [99]. The treated surfaces were characterized in terms of surface roughness ($R_a$), WCA, microhardness, and chemical composition in the treated surfaces. LST of PP resulted in the melting of the surface, along with the adhesion of carbon particles on its surface. The final roughness ($R_a$) was found to be higher than 1 µm, which is considered the minimum required value to improve the bone/implant bonding degree [100]. Moreover, ATR-FTIR analyses revealed the formation of carbonyl (C=O) and hydroxyl (C-O) groups on the treated surfaces. The formation of polar groups, along with the increase of the $R_a$ above 1 µm, enhance the adhesion properties of PP surfaces. These findings suggest a better biological response; however, a biological characterization of laser textured PP surfaces is absent in this work.

Buchman et al. obtained analogous results using similar laser wavelengths ($\lambda = 1{,}064$, 535, 350, and 266 nm) produced by a Nd:YAG laser [58]. In this case, micro-structures (which can serve as anchoring points to promote the cell adhesion) were produced in the surface of the samples (especially, during 1,064 nm laser irradiation). They also found an oxidation of the surface as a result of the treatment. This promotes the activation of the surface and enables chemical bonding to the treated PP.

Murahara and Okoshi followed a different approach to increase the wettability of PP [56]. This material was irradiated in the presence of tap water by a laser beam produced by an ArF laser. The treatment with UV radiation is able to pull out H atoms, and they were replaced with OH functional groups (in this aqueous environment). This reduces the well-known chemical stability of PP, attributed to the C-H and C-$H_3$ bonds. The measurement of the contact angle showed a minimum (contact

angle for base material: 93°, and minimum angle for the laser treated surfaces 65°) for a certain fluence and shot number (laser fluence of 12.5 mJ/cm$^2$ and a shot number of 10,000). In this case, the hydrophilic behavior showed after the treatment was exclusively attributed to the presence of OH groups on the surface of the treated areas. Khaledian et al. [59] also observed the formation of polar functional groups on PP (and in chitosan) surfaces irradiated with UV laser radiation ($\lambda = 248$ nm). Their presence explained the increase in the WCA after the laser treatment. They also studied the influence of the topography on the cell viability. Two kind of surfaces, oriented, and non-oriented surfaces, were evaluated. Oriented topographies showed a higher viability than non-oriented surfaces; however, in both cases, cell viability was higher than in non laser-treated PP surfaces.

## Polyethylene (PE)

Polyethylene (PE) is a synthetic thermoplastic polymer, bioinert, and non-biodegradable in contact with corporal fluids. Among the typical implant applications of this material, chin, cheek, and jaw reconstruction should be highlighted [101]. LST has been applied to this material given to its inertness [62, 63, 102].

Okoshi and Inoue studied the utilization of fs laser sources to ablate and modify the surface of PE samples [62, 102]. The effect of the laser wavelength on the surface topography and chemistry was addressed. LST on PE was performed with a fs Ti:Sapphire laser source using 790 nm laser light, and second harmonics 395 nm. Both wavelengths were found to successfully ablate PE surfaces. The ablation threshold for the 790 nm wavelength was ∼50 mJ/cm$^2$, while for 395 nm was 17 mJ/cm$^2$ [62]. Comparing wavelengths, 395 nm second harmonics etched PE faster. This was attributed to the higher energetic photons of this laser wavelength compared to those involving 790 nm. In terms of chemical composition, ablated surfaces presented novel carbonyl (C=O) polar groups [102]. Yi and Feng evaluated the effect of a second harmonics 532 nm Nd:YAG laser source (pulse duration = 10 ns) on the surface ablation of PE substrates [60]. It was found that the ablated surface appeared different in this case, given the high crystallinity of PE compared to the other investigated amorphous polymers [e.g., Poly(methyl methacrylate) (PMMA)]. Isolated particles at the bottom of spots appeared, and no rims were detected. Dadbin studied the $CO_2$ laser modification of the wettability of low-density polyethylene (LDPE) surface films in pulsed mode [61]. This laser wavelength also induces both topography and surface chemistry variations in PE surfaces.

The biological performance of PE laser textured surfaces was evaluated after being subjected to Nd:YAG laser radiation ($\lambda = 1{,}064$ nm) by Blanchemain et al. [63]. For this purpose, roughness, wettability, chemistry, and cell viability tests were performed. After laser irradiation, the surface roughness of PE was increased up to a value of $R_a = 0.2\,\mu$m. XPS results indicated that after laser exposition the surface exhibited new polar groups (e.g., hydroxyl, C–OH), and a higher oxidation state; however, it was not found a significant change in the wettability of PE before, and after LST. Cell viability tests were performed to evaluate the cytotoxicity of laser irradiated PE. *In vitro* tests were conducted using human embryonic pulmonary epithelial cells (L132 cell line). Results revealed enhancement in cell adhesion and proliferation of irradiated PE surfaces compared to pristine ones. A greater spreading of the cells (which showed large lamellipodia) was noticed on the laser-treated surfaces. These findings were attributed to the chemical modifications of the surface, along with the increase in the average roughness on the PE surfaces.

## Polycarbonate (PC)

Polycarbonate (PC) is an amorphous thermoplastic polymer exhibiting high transparency to visible light. It presents adequate mechanical properties, as well as biostability, which make it a suitable material to be used for biomedical applications. PC has been used as biomaterial with applications ranging between renal dialysis to cardiac surgery [103].

In the last decades, different laser wavelengths were studied to assess their effect on the surface properties of textured PC, ranging from UV ($\lambda = 248$ nm) to NIR ($\lambda = 1{,}064$ nm). On the other hand, to the best of our knowledge, LST of this polymer was found to be performed using solely ns laser sources.

Viville et al. were the first performing LST on PC, more specifically, on PC/PMMA blends [64]. This study was conducted with the aim to evaluate physical and chemical modifications of the laser treated surfaces. A UV laser beam (with a pulse length of 30 ns) emitted by a KrF excimer laser was employed for such application. It was demonstrated the ability of UV radiation to generate micropatterns, and chemical modifications on PC/PMMA blend surfaces. Regarding the chemical composition after UV laser irradiation, a more detailed study was performed by Ahad et al. using a laser-plasma extreme ultraviolet (EUV) source [103]. XPS analysis revealed a decrease in the surface oxygen content after laser processing, which resulted in an increase of the hydrophobicity of the PC surface. Conversely, Laurens et al. reported opposite results with similar processing conditions ($\lambda = 193$ and 248 nm, and pulse duration = 20 and 30 ns) [65]. UV laser radiation induced the oxidation, and the formation of polar groups on the surface of the samples. The creation of new carboxyl (O-C=O) and peroxide (O-O) groups was attributed to scission of initial bonds of PC under the irradiation of high energetic UV photons, and further reactions forming radicals given the oxygenated environment [65].

The evaluation of the cell viability of PC surfaces after LST was conducted by Ramazani et al. [66]. A pulsed Nd:YAG laser source ($\lambda = 355$ and 1,064 nm, and pulse duration of 10 ns) was used to modify PC substrates. Roughness, wettability, and cell viability (using mouse L929 fibroblast cells) were evaluated after the processing. With regard to the topography, the 1064 nm laser radiation produced the thermal degradation of the material. However, by exposing PC to 355 nm radiation, photodegradation was identified as the mechanism of the surface modification. The roughness increased in both cases; however, the wettability was substantially increased for the 1,064 nm laser radiation (the contact angle evolved from 70° for the base material, up to 40° for the treated surfaces), while it remained unaltered for the 355 nm laser treatment. The chemical characterization of the treated surfaces revealed an increase in the formation of polar groups

(principally carbonyl groups). These findings can be related to the enhancement of cell attachment and proliferation. The formation of polar groups increased the cell viability. SEM images confirmed an increase in the cell growth after laser exposition of PC. It was noticed that the application of a lower laser energy density also reduces the cell growth. Authors also pointed out that the 1,064 nm laser radiation induces a more efficient cell growth than the 355 nm laser irradiation. This was attributed to the inhomogeneous modification of the surface by the 355 nm radiation (probably due to the utilization of an inhomogeneous laser beam).

## Other Polymers

Other polymers have also been investigated to enhance their biocompatibility using laser texturing techniques. In this regard, polytetrafluoroethylene (PTFE) was modified by UV laser [104]. Ahad et al. performed the process in a nitrogen-rich environment. The treatment resulted in an accurately controlled surface patterning. Regarding the chemical modification, the detachment of fluorine, the shortening of the polymer chains, and the formation of C=C and other bonds between C, O, and N, would explain the observed increment of the O/C ratio, and the reduction of the F/C ratio with the number of laser pulses. In terms of cell viability, it was demonstrated the ability of the process to improve cell adhesion, along with a good cell morphology [104].

Another thermoplastic such as nylon 6,6 was also textured using a $CO_2$ laser to enhance its biocompatibility [67]. The biological studies revealed that the surface modification using this laser wavelength affected on the cell viability of nylon. Cell growth was improved on $CO_2$ laser-treated surfaces. Osteoblast cells covered more area in the textured surfaces compared to the pristine ones.

Polyimide (PI) was textured using different laser wavelengths ($\lambda$ = 1,064, 532, 355, and 266 nm) to avoid the biofilm formation on indwelling medical devices [105]. Several topographies were tested against *Staphylococcus aureus* adhesion. Line- and pillar-like patterns were noticed to promote the adhesion of this pathogen. On the contrary, lamella micro-topographies reduced the adhesion in both static and continuous flow culture conditions. These textured showed also the capacity to inhibit the adhesion of this pathogen also when it was subcutaneously implanted. However, more research is necessary to validate that this kind of topography can also inhibit *S. aureus* adhesion on the surface of other polymers.

De Marco et al. conducted experiments using a fs Ti:Sapphire laser source ($\lambda$ = 800 nm and pulse duration of 150 fs) to evaluate the wettability changes on poly(methyl methacrylate) (PMMA) after the laser treatment [72]. They also proposed this technique to fabricate microchannels with controlled, size, and roughness for microfluidics applications. Regarding wettability, it was observed an increase in the WCA. The presence of debris after the laser treatment reduced the contact angle from 74.1° (for the base material), up to 20° approximately; however, the removal of the debris, after rinsing and drying the surface, increased the contact angle up to 94°. This fact was attributed to the double-scale roughness topographies created after ablation, which turn the surface into an intermediate state between the Wenzel [14], and Cassie and Baxter [15] states. Chemical analyses did not revealed surface alteration on the ablated surface. This supported the aforementioned explanation for the wettability change. Wang et al. also used fs laser radiation on PMMA samples. They were able to obtain different wetting behaviors controlling the laser fluence [74]. WCAs ranging from ∼0 to 125° were successfully achieved in this way. When the laser fluence ranged between 0.4 and 2.5 J/cm$^2$, a hydrophobic behavior was detected. However, the surface became hydrophilic with the increment of the laser fluence due to the formation of more polar groups (O-C, O=C). These features may be beneficial for the cell attachment and proliferation on PMMA modified surfaces, which make fs lasers a viable alternative to enhance biocompatibility. Deepak et al. [73, 75, 106, 107] also explored the utilization of Ti:Sapphire femtosecond lasers to produce microchannels in PMMA, and also in polystyrene (PS) for microfluidic applications (with potential biomedical applications). Peroxide-type free radicals where found along the laser treated areas. Although no cell culture assays were performed, the presence of these radicals may not affect the cells used in these microfluidic devices, as they are only present on the walls of the channels. Pfleging et al. [71] studied the influence of the processing atmosphere on the wettability during laser treatment with UV radiation ($\lambda$ = 193 nm). It was found a marked decrease of the WCA when $O_2$ is used as processing gas. This was attributed to the oxidation of the surface. On the other hand, Waugh et al. [68] evaluated the biological performance of PMMA samples textured with IR laser radiation ($\lambda$ = 10,600 nm). An increase in the surface roughness is observed with the laser power, and the distance between textured grooves. Cell viability tests (performed with osteoblast and mesenchymal stem cells) demonstrated a superior cell growth on the laser-treated surfaces. These results were attributed to the increment in the surface roughness and surface oxygen content.

# CHALLENGES AND FUTURE TRENDS

The present work highlights the excellent performance of laser texturing for tailoring the biological performance of biomedical polymers; however, several issues remain unanswered, and the way to real applications is still challenging.

The first challenge is the lack of *in vivo* tests supporting the better biological performance observed in the laser-treated polymers. Several works addressed the *in vitro* performance of materials. They showed the better cell response of laser-textured materials; however, not enough animal studies, or clinical trials are found in the literature to support these studies and move this technology into real applications. Another important issue is related to the textured topographies. The most efficient pattern for a specific biomedical application cannot be ascertained from the works found in the literature. This problem is also related to how cells react with the substrate, and how this can be used to elicit a desired cell response (see, for example the work done by Bettinger et al. [11]). Another related issue is that in most of the research works only the microtopographies produced by the laser treatment are analyzed. Laser texturing does not only modify the

surface at the micrometer scale, but also at the nanometric scale. At the same time, it should be clarified if the surface chemistry is also modified at the nanometric scale i.e., it should be answered if the surface chemistry is homogeneously modified by the laser treatments (even at the nanometric scale). These challenges can stimulate the future research in different ways.

Up to now, LST has been studied to demonstrate the superior biocompatibility of laser-textured polymers; however, less attention has been paid to the possibilities of this technique to avoid the biofilm formation on these surfaces. Bacterial colonization and biofilm formation is a serious problem in long-term implanted or intravascular devices [108]. These infections lead to significant pain and distress in patients, and can require implant revision surgery. It has been demonstrated that roughness and wettability are critical factors on the bacterial colonization [109]. Therefore, LST can be applied to polymeric biomaterials to address this problem. This approach has been recently applied on metals (see e.g., [110–112]). This application is not only interesting for biomedical applications, but also in the food industry.

Other potential application of LST for biomedical applications is the surface texturing of polymeric surfaces to control and regulate stem cell differentiation and maturation on polymeric biomaterials. Some works demonstrated the impact of wettability and roughness on directing mesenchymal stem cells toward the osteogenic lineage. Therefore, the osteogenic lineage fate can be modulated by means of suitable surface characteristics of topography and wettability [113–116]. Using LST, exogenous soluble factors could be avoided.

LST has been mainly studied on common polymers, but treatment of composites for biomedical applications have not been extensively studied. Researchers should perform studies in more polymers, and composites to extract general conclusions on aspects such as: the determination of the optimum laser wavelength for each material, or even the processing conditions required for the optimum modification of any surface topography, chemistry or both. Research studies reviewed in this work also highlight that only one laser wavelength was applied each time. It has not been tested the joint effect of two and more different laser wavelengths (e.g., one suitable to tailor the surface roughness, and other suitable to tailor the surface chemistry). Finally, a major task could be the computer design of surfaces (as it is routinely done in the manufacturing sector) to elicit a certain cell or bacteria response given a certain polymer or composite for the intended application. This would require more work on the field of the simulation of laser texturing process of polymers (issue initially addressed by Conde et al. using a finite element method approach [117]).

## CONCLUSIONS

This work has demonstrated the potential of LST to tailor the biological performance of polymers currently used in the clinical practice. This is done by the modification of the surface roughness, chemistry, or both at the same time. This technique is clean, versatile, has a high temporal and spatial resolution, highly efficient, and can be performed avoiding the presence of toxic chemicals. Although there is still a long way to make this technique a standard tool in the biomedical industry, the results found in the literature are very promising and demonstrate the potential application of LST to address some drawbacks exhibited by these materials within the field of biomedical implants fields.

## AUTHOR CONTRIBUTIONS

AR and AM: Conceived the study, and wrote the manuscript. JdV and RC: Helped to evaluate and edit the manuscript. JP: Supervised the development of work, helped in data interpretation, and manuscript evaluation.

## ACKNOWLEDGMENTS

This work was partially supported by the EU research project Bluehuman (EAPA_151/2016 Interreg Atlantic Area), Government of Spain [MAT2015-71459-C2-P (MINECO/FEDER), PRX17/00157], and by Xunta de Galicia (ED431B 2016/042 (GPC), and Plan I2C Grant Program POS-A/2013/161, ED481B 2016/047-0, ED481D 2017/010).

## REFERENCES

1. Parithimarkalaignan S, Padmanabhan TV. Osseointegration: an update. *J Indian Prosthodont Soc*. (2013) **13**:2–6. doi: 10.1007/s13191-013-0252-z
2. Dee KC, Puleo DA, Bizios R. *An Introduction to Tissue-Biomaterial Interactions*. Hoboken, NJ: John Wiley & Sons (2003).
3. Tanner KE. Bioactive ceramic-reinforced composites for bone augmentation. *J R Soc Interface* (2010) **7**:S541–57. doi: 10.1098/rsif.2010.0229.focus
4. Bosco R, Van Den Beucken J, Leeuwenburgh S, Jansen J. Surface engineering for bone implants: a trend from passive to active surfaces. *Coatings* (2012) **2**:95–119. doi: 10.3390/coatings2030095
5. Ma R, Tang T. Current strategies to improve the bioactivity of PEEK. *Int J Mol Sci*. (2014) **15**:5426–45. doi: 10.3390/ijms15045426
6. Durham JW III, Montelongo SA, Ong JL, Guda T, Allen MJ, Rabiei A. Hydroxyapatite coating on PEEK implants: biomechanical and histological study in a rabbit model. *Mater Sci Eng C* (2016) **68**:723–31. doi: 10.1016/j.msec.2016.06.049
7. Kaiser JP, Bruinink A. Investigating cell–material interactions by monitoring and analysing cell migration. *J Mater Sci Mater Med*. (2004) **15**:429–35. doi: 10.1023/B:JMSM.0000021115.55254.a8
8. Alla RK, Ginjupalli K, Upadhya N, Shammas M, Ravi RK, Sekhar R. Surface roughness of implants: a review. *Trends Biomater Artif Organs* (2011) **25**:112–8.
9. Dahiya V, Shukla P, Gupta S. Surface topography of dental implants: a review. *J Dent Implants* (2014) **4**:66. doi: 10.4103/0974-6781.131009
10. Gittens RA, Olivares-Navarrete R, Schwartz Z, Boyan BD. Implant osseointegration and the role of microroughness and nanostructures: lessons for spine implants. *Acta Biomater*. (2014) **10**:3363–71. doi: 10.1016/j.actbio.2014.03.037
11. Bettinger CJ, Langer R, Borenstein JT. Engineering substrate topography at the micro- and nanoscale to control cell function. *Angew. Chem Int Ed*. (2009) **48**:5406–15. doi: 10.1002/anie.200805179
12. Schakenraad JM, Busscher HJ, Wildevuur CRH, Arends J. The influence of substratum surface free energy on growth and spreading of human

fibroblasts in the presence and absence of serum proteins. *J Biomed Mater Res*. (1986) **20**:773–84. doi: 10.1002/jbm.820200609
13. Baier RE. Surface behaviour of biomaterials: the theta surface for biocompatibility. *J Mater Sci Mater Med*. (2006) **17**:1057. doi: 10.1007/s10856-006-0444-8
14. Wenzel RN. Resistance of solid surfaces to wetting by water. *Ind Eng Chem*. (1936) **28**:988–94. doi: 10.1021/ie50320a024
15. Cassie ABD, Baxter S. Wettability of porous surfaces. *Trans Faraday Soc*. (1944) **40**:546–51. doi: 10.1039/tf9444000546
16. de Gennes PG, Brochard-Wyart F, Quere D. *Capillarity and Wetting Phenomena: Drops, Bubbles, Pearls, Waves*. New York, NY: Springer Science & Business Media (2013).
17. Siow KS, Britcher L, Kumar S., Griesser HJ. Plasma methods for the generation of chemically reactive surfaces for biomolecule immobilization and cell colonization - a review. *Plasma Process Polym*. (2006) **3**:392–418. doi: 10.1002/ppap.200600021
18. Ratner BD. Surface modification of polymers: chemical, biological and surface analytical challenges. *Biosens Bioelectron*. (1995) **10**:797–804. doi: 10.1016/0956-5663(95)99218-A
19. Wakelin EA, Fathi A, Kracica M, Yeo GC, Wise SG, Weiss AS, et al. Mechanical properties of plasma immersion ion implanted PEEK for bioactivation of medical devices. *ACS Appl Mater Interfaces* (2015) **7**:23029–40. doi: 10.1021/acsami.5b06395
20. del Campo A, Arzt E. Fabrication approaches for generating complex micro- and nanopatterns on polymeric surfaces. *Chem. Rev*. (2008) **108**:911–45. doi: 10.1021/cr050018y
21. Lippert T. Laser application of polymers. *Adv Polym Sci*. (2004) **168**:51–246. doi: 10.1007/b12682
22. Bereznai M, Pelsöczi I, Tóth Z, Turzó K, Radnai M, Bor Z, et al. Surface modifications induced by ns and sub-ps excimer laser pulses on titanium implant material. *Biomaterials* (2003) **24**:4197–203. doi: 10.1016/S0142-9612(03)00318-1
23. Gaggl A, Schultes G, Müller WD, Kärcher H. Scanning electron microscopical analysis of laser-treated titanium implant surfaces-a comparative study. *Biomaterials* (2000) **21**:1067–73. doi: 10.1016/S0142-9612(00)00002-8
24. Ranella A, Barberoglou M, Bakogianni S, Fotakis C, Stratakis E. Tuning cell adhesion by controlling the roughness and wettability of 3D micro/nano silicon structures. *Acta Biomater*. (2010) **6**:2711–20. doi: 10.1016/j.actbio.2010.01.016
25. Lippert T, Dickinson JT. Chemical and spectroscopic aspects of polymer ablation: special features and novel directions. *Chem Rev*. (2003) **103**:453–85. doi: 10.1021/cr010460q
26. Lippert T. Interaction of photons with polymers: from surface modification to ablation. *Plasma Process Polym*. (2005) **2**:525–46. doi: 10.1002/ppap.200500036
27. Lippert T. UV laser ablation of polymers: from structuring to thin film deposition. In: Miotello A, Ossi PM, editors. *Laser-Surface Interactions for New Materials Production Springer Series in Materials Science*. Berlin; Heidelberg: Springer (2010). p. 141–75.
28. Etsion I. State of the art in laser surface texturing. *J Tribol*. (2005) **127**:248–53. doi: 10.1115/1.1828070
29. Tan WS, Zhou JZ, Huang S, Zhu WL, Meng XK. Fabrication of polymer microcomponents using CO2 laser melting technique. *Polimery/Polymers* (2015) **60**:192–8. doi: 10.14314/polimery.2015.192
30. Wong W, Chan K, Yeung KW, Lau KS. Chemical surface modification of poly (ethylene terephthalate) by excimer irradiation of high and low intensities. *Mater Res Innov*. (2001) **4**:344–9. doi: 10.1007/s100190000116
31. Bäuerle DW. *Laser Processing and Chemistry*. Berlin; Heidelberg: Springer Science & Business Media (2013).
32. Makropoulou M, Serafetinides AA, Skordoulis CD. Ultra-violet and infra-red laser ablation studies of biocompatible polymers. *Lasers Med Sci*. (1995) **10**:201–6. doi: 10.1007/BF02133332
33. Serafetinides AA, Makropoulou MI, Skordoulis CD, Kar AK. Ultra-short pulsed laser ablation of polymers. *Appl Surf Sci*. (2001) **180**:42–56. doi: 10.1016/S0169-4332(01)00324-5
34. Bityurin N, Luk'yanchuk BS, Hong MH, Chong TC. Models for laser ablation of polymers. *Chem Rev*. (2003) **103**:519–52. doi: 10.1021/cr010426b
35. Chen S, Kancharla VV, Lu Y. Laser-based microscale patterning of biodegradable polymers for biomedical applications. *Int J Mater Prod Technol*. (2003) **18**:457–68. doi: 10.1504/IJMPT.2003.002502
36. Krüger J, Kautek W. Ultrashort pulse laser interaction with dielectrics and polymers. *Adv Polym Sci*. (2004) **168**:247–89. doi: 10.1007/b12683
37. Bityurin N. Studies on laser ablation of polymers. *Annu Rep Prog Chem*. (2005) **101**:216–47. doi: 10.1039/b408910n
38. Han A, Pillon G, Nichici A, Gubencu D, Grevey D, Cicala E. Study of polymer laser grooving using a complete factorial experiment. *Lasers Eng*. (2005) **15**:215–31.
39. Eaton SM, De M, Martinez-Vazquez R, Ramponi R, Turri S, Cerullo G, et al. Femtosecond laser microstructuring for polymeric lab-on-chips. *J Biophotonics* (2012) **5**:687–702. doi: 10.1002/jbio.201200048
40. Bityurin NM. Laser nanostructuring of polymers. In: Veiko VP, Konov VI, editors. *Fundamentals of Laser-Assisted Micro- and Nanotechnologies Springer Series in Materials Science*. Cham: Springer (2014). p. 293–313.
41. Rao SV, Podagatlapalli GK, Hamad S. Ultrafast laser ablation in liquids for nanomaterials and applications. *J Nanosci Nanotechnol*. (2014) **14**:1364–88. doi: 10.1166/jnn.2014.9138
42. Lawrence J, Li L. Modification of the wettability characteristics of polymethyl methacrylate (PMMA) by means of CO2, Nd:YAG, excimer and high power diode laser radiation. *Mater Sci Eng A* (2001) **303**:142–9. doi: 10.1016/S0921-5093(00)01851-7
43. Laurens P, Sadras B, Decobert F, Arefi-Khonsari F, Amouroux J. Enhancement of the adhesive bonding properties of PEEK by excimer laser treatment. *Int J Adhes Adhes*. (1998) **18**:19–27. doi: 10.1016/S0143-7496(97)00063-8
44. Riveiro A, Soto R, Comesa-a R, Boutinguiza M, Del V, Quintero F, et al. Laser surface modification of PEEK. *Appl Surf Sci*. (2012) **258**:9437–42. doi: 10.1016/j.apsusc.2012.01.154
45. Bremus-Koebberling EA, Beckemper S, Koch B, Gillner A. Nano structures via laser interference patterning for guided cell growth of neuronal cells. *J Laser Appl*. (2012) **24**:042013. doi: 10.2351/1.4730804
46. Cordero D, López-Álvarez M, Rodríguez-Valencia C, Serra J, Chiussi S, González P. *In vitro* response of pre-osteoblastic cells to laser microgrooved PEEK. *Biomed Mater*. (2013) **8**:055006. doi: 10.1088/1748-6041/8/5/055006
47. Zheng Y, Xiong C, Wang Z, Li X, Zhang L. A combination of CO2 laser and plasma surface modification of poly(etheretherketone) to enhance osteoblast response. *Appl Surf Sci*. (2015) **344**:79–88. doi: 10.1016/j.apsusc.2015.03.113
48. Wilson A, Jones I, Salamat-Zadeh F, Watts JF. Laser surface modification of poly(etheretherketone) to enhance surface free energy, wettability and adhesion. *Int J Adhes Adhes*. (2015) **62**:69–77. doi: 10.1016/j.ijadhadh.2015.06.005
49. Michaljaničová I, Slepička P, Rimpelová S, Slepičková Kasálková N, Švorčík V. Regular pattern formation on surface of aromatic polymers and its cytocompatibility. *Appl Surf Sci*. (2016) **370**:131–41. doi: 10.1016/j.apsusc.2016.02.160
50. Guo J, Liu L, Liu H, Gan K, Liu X, Song X, et al. Influence of femtosecond laser on the osteogenetic efficiency of polyetheretherketone and its composite. *High Perform Polym*. (2017) **29**:997–1005. doi: 10.1177/0954008316667460
51. Lorusso A, Nassisi V, Paladini F, Torrisi L, Visco AM, Campo N. Comparison of the laser effects induced on ultra-high-molecular-weight polyethylene. *Radiat Eff Defects Solids* (2008) **163**:435–40. doi: 10.1080/10420150701778155
52. Torrisi L, Visco AM, Campo N, Caridi F. Pulsed laser treatments of polyethylene films. *Nucl Instrum Methods Phys Res B Beam Interact Mater Atoms* (2010) **268:**3117–21. doi: 10.1016/j.nimb.2010.05.067
53. Velardi L, Lorusso A, Paladini F, Siciliano MV, Giulio MD, Rainò A, et al. Modification of polymer characteristics by laser and ion beam. *Radiat Eff Defects Solids* (2010) **165**:637–42. doi: 10.1080/10420151003729516
54. Fernández-Pradas JM, Naranjo-León S, Morenza JL, Serra P. Surface modification of UHMWPE with infrared femtosecond laser. *Appl Surf Sci*. (2012) **258**:9256–9. doi: 10.1016/j.apsusc.2011.09.106
55. Riveiro A, Soto R, del Val J, Comesa-a R, Boutinguiza M, Quintero F, et al. Laser surface modification of ultra-high-molecular-weight polyethylene (UHMWPE) for biomedical applications. *Appl Surf Sci*. (2014) **302**:236–42. doi: 10.1016/j.apsusc.2014.02.130

56. Murahara M, Okoshi M. Photochemical surface modification of polypropylene for adhesion enhancement by using an excimer laser. *J Adhes Sci Technol*. (1995) **9**:1593–9. doi: 10.1163/156856195X00220
57. Belaud V, Valette S, Stremsdoerfer G, Beaugiraud B, Audouard E, Benayoun S. Femtosecond laser ablation of polypropylene: a statistical approach of morphological data. *Scanning* (2014) **36**:209–17. doi: 10.1002/sca.21090
58. Buchman A, Rotel M, Dodiuk-Kenig H. Nd:YAG laser surface treatment of various materials to enhance adhesion. In: Mittal KL, Bahners T, editors. *Laser Surface Modification and Adhesion*. John Wiley & Sons, Inc.; Scrivener Publishing LLC (2014) p. 1–53.
59. Khaledian M, Jiroudhashemi F, Biazar E. Chitosan- and polypropylene-oriented surface modification using excimer laser and their biocompatibility study. *Artif Cells Nanomed Biotechnol*. (2017) **45**:135–8. doi: 10.3109/21691401.2016.1138485
60. Yi XSU, Feng Y. Etching behavior of plastics using a near infrared laser. *J Mater Sci Lett*. (1999) **18**:245–7. doi: 10.1023/A:1006690029986
61. Dadbin S. Surface modification of LDPE film by CO2 pulsed laser irradiation. *Eur Polym J*. (2002) **38**:2489–95. doi: 10.1016/S0014-3057(02)00134-9
62. Okoshi M, Inoue N. Microfabrication of polyethylene using femtosecond Ti:sapphire laser and nanosecond ArF laser. *Jpn J Appl Phys*. (2003) **42**:5642. doi: 10.1143/JJAP.42.5642
63. Blanchemain N, Chai F, Bacquet M, Gengembre L, Traisnel M, Setti Y, et al. Improvement of biological response of YAG laser irradiated polyethylene. *J Mater Chem*. (2007) **17**:4041–9. doi: 10.1039/b708250a
64. Viville P, Beauvois S, Lambin G, Lazzaroni R, Brédas JL, Kolev K, et al. Excimer laser-induced surface modifications of biocompatible polymer blends. *Appl Surf Sci*. (1996) **96**:558–562. doi: 10.1016/0169-4332(95)00530-7
65. Laurens P, Ould Bouali M, Meducin F, Sadras B. Characterization of modifications of polymer surfaces after excimer laser treatments below the ablation threshold. *Appl Surf Sci*. (2000) **154–155:**211–6. doi: 10.1016/S0169-4332(99)00443-2
66. Ramazani SA, Mousavi SA, Seyedjafari E, Poursalehi R, Sareh S, Silakhori K, et al. Polycarbonate surface cell's adhesion examination after Nd:YAG laser irradiation. *Mater Sci Eng C* (2009) **29**:1491–7. doi: 10.1016/j.msec.2008.11.019
67. Waugh DG, Lawrence J, Morgan DJ, Thomas CL. Interaction of CO2 laser-modified nylon with osteoblast cells in relation to wettability. *Mater Sci Eng C* (2009) **29**:2514–24. doi: 10.1016/j.msec.2009.07.020
68. Waugh DG, Lawrence J, Shukla P. Modulating the wettability characteristics and bioactivity of polymeric materials using laser surface treatment. *J Laser Appl*. (2016) **28:**022502. doi: 10.2351/1.4944441
69. Langheinrich D, Yslas E, Broglia M, Rivarola V, Acevedo D, Lasagni A. Control of cell growth direction by direct fabrication of periodic micro- and submicrometer arrays on polymers. *J Polym Sci Part B Polym Phys*. (2012) **50:**415–22. doi: 10.1002/polb.23017
70. Lasagni AF, Acevedo DF, Barbero CA, Mücklich F. One-step production of organized surface architectures on polymeric materials by direct laser interference patterning. *Adv Eng Mater*. (2007) **9**:99–103. doi: 10.1002/adem.200600171
71. Pfleging W, Adamietz R, Brückner HJ, Bruns M, Welle A. Laser-assisted modification of polymers for microfluidic, micro-optics, and cell culture applications. In: *International Society for Optics and Photonics*. San Jose, CA: EE.UU (2007). p. 645907.
72. De Marco C, Eaton SM, Suriano R, Turri S, Levi M, Ramponi R, et al. Surface Properties of femtosecond laser ablated PMMA. *ACS Appl Mater Interfaces* (2010) **2**:2377–84. doi: 10.1021/am100393e
73. Kallepalli DLN, Desai NR, Soma VR. Fabrication and optical characterization of microstructures in poly(methylmethacrylate) and poly(dimethylsiloxane) using femtosecond pulses for photonic and microfluidic applications. *Appl Opt*. (2010) **49**:2475–89. doi: 10.1364/AO.49.002475
74. Wang ZK, Zheng HY, Xia HM. Femtosecond laser-induced modification of surface wettability of PMMA for fluid separation in microchannels. *Microfluid Nanofluidics* (2011) **10**:225–9. doi: 10.1007/s10404-010-0662-8
75. Kallepalli LN, Desai NR, Rao SV. Femtosecond-laser direct writing in polymers and potential applications in microfluidics and memory devices. *Opt Eng*. (2012) **51**:073402. doi: 10.1117/1.OE.51.7.073402
76. Momma C, Nolte S, Chichkov BN, Alvensleben Fv, Tünnermann A. (1997). Precise laser ablation with ultrashort pulses. *Appl Surf Sci.* **109–110:**15–9. doi: 10.1016/S0169-4332(96)00613-7
77. Hallab NJ, Jacobs JJ. Biologic effects of implant debris. Bulletin of the NYU hospital for joint diseases. *Bull NYU Hosp Jt Dis*. (2009) **67**:182–8.
78. Küper S, Stuke M. Ablation of polytetrafluoroethylene (Teflon) with femtosecond UV excimer laser pulses. *Appl Phys Lett*. (1989) **54**:4–6. doi: 10.1063/1.100831
79. Alamri S, Aguilar-Morales AI, Lasagni AF. Controlling the wettability of polycarbonate substrates by producing hierarchical structures using Direct Laser Interference Patterning. *Eur Polym J*. (2018) **99**:27–37. doi: 10.1016/j.eurpolymj.2017.12.001
80. Borchers B, Bekesi J, Simon P, Ihlemann J. Submicron surface patterning by laser ablation with short UV pulses using a proximity phase mask setup. *J Appl Phys*. (2010) **107**:063106. doi: 10.1063/1.3331409
81. Jagur-Grodzinski J. Polymers for tissue engineering, medical devices, and regenerative medicine. Concise general review of recent studies. *Polym Adv Technol*. (2006) **17**:395–418. doi: 10.1002/pat.729
82. Kohane DS, Langer R, Langer R. Polymeric biomaterials in tissue engineering. *Pediatr Res*. (2008) **63**:487–91. doi: 10.1203/01.pdr.0000305937.26105.e7
83. Teo AJT, Mishra A, Park I, Kim YJ, Park WT, Yoon YJ. Polymeric biomaterials for medical implants and devices. *ACS Biomater Sci Eng*. (2016) **2**:454–72. doi: 10.1021/acsbiomaterials.5b00429
84. Maitz MF. Applications of synthetic polymers in clinical medicine. *Biosurface Biotribol*. (2015) **1**:161–76. doi: 10.1016/j.bsbt.2015.08.002
85. Abu Bakar MS, Cheng MHW, Tang SM, Yu SC, Liao K, Tan CT, et al. Tensile properties, tension–tension fatigue and biological response of polyetheretherketone–hydroxyapatite composites for load-bearing orthopedic implants. *Biomaterials* (2003) **24**:2245–50. doi: 10.1016/S0142-9612(03)00028-0
86. Godara A, Raabe D, Green S. The influence of sterilization processes on the micromechanical properties of carbon fiber-reinforced PEEK composites for bone implant applications. *Acta Biomater*. (2007) **3**:209–20. doi: 10.1016/j.actbio.2006.11.005
87. Riveiro A, Soto R, del Val J, Comesa-a R, Boutinguiza M, Quintero F, et al. Texturing of polypropylene (PP) with nanosecond lasers. *Appl Surf Sci*. (2016) **374**:379–86. doi: 10.1016/j.apsusc.2016.01.206
88. Briski DC, Cook BW, Zavatsky JM, Ganey T. Laser modified PEEK implants as an adjunct to interbody fusion: a sheep model. *Spine J*. (2015) **15**:S187. doi: 10.1016/j.spinee.2015.07.242
89. Torrisi L, Gammino S, Mezzasalma AM, Visco AM, Badziak J, Parys P, et al. Laser ablation of UHMWPE-polyethylene by 438 nm high energy pulsed laser. *Appl Surf Sci*. (2004) **227**:164–74. doi: 10.1016/j.apsusc.2003.11.078
90. Ramakrishna S, Mayer J, Wintermantel E, Leong KW. Biomedical applications of polymer-composite materials: a review. *Compos Sci Technol*. (2001) **61**:1189–224. doi: 10.1016/S0266-3538(00)00241-4
91. Grubova IY, Surmeneva MA, Shugurov VV, Koval NN, Selezneva II, Lebedev SM, et al. Effect of electron beam treatment in air on surface properties of ultra-high-molecular-weight polyethylene. *J Med Biol Eng*. (2016) **36**:440–8. doi: 10.1007/s40846-016-0135-y
92. Himma NF, Anisah S, Prasetya N, Wenten IG. Advances in preparation, modification, and application of polypropylene membrane. *J Polym Eng*. (2016) **36**:329–62. doi: 10.1515/polyeng-2015-0112
93. Erbil HY, Demirel AL, Avci Y, Mert O. Transformation of a simple plastic into a superhydrophobic surface. *Science* (2003) **299**:1377–80. doi: 10.1126/science.1078365
94. Cui NY, Brown NMD. Modification of the surface properties of a polypropylene (PP) film using an air dielectric barrier discharge plasma. *Appl Surf Sci*. (2002) **189**:31–8. doi: 10.1016/S0169-4332(01)01035-2
95. Lai J, Sunderland B, Xue J, Yan S, Zhao W, Folkard M, et al. Study on hydrophilicity of polymer surfaces improved by plasma treatment. *Appl Surf Sci*. (2006) **252**:3375–9. doi: 10.1016/j.apsusc.2005.05.038
96. Shim JK, Na HS, Lee YM, Huh H, Nho YC. Surface modification of polypropylene membranes by γ-ray induced graft copolymerization and their solute permeation characteristics. *J Membr Sci*. (2001) **190**:215–26. doi: 10.1016/S0376-7388(01)00445-8

97. Myllymaa K, Myllymaa S, Korhonen H, Lammi MJ, Saarenpää H, Suvanto M, et al. Improved adherence and spreading of Saos-2 cells on polypropylene surfaces achieved by surface texturing and carbon nitride coating. *J Mater Sci Mater Med*. (2009) **20**:2337. doi: 10.1007/s10856-009-3792-3
98. Belaud V, Valette S, Stremsdoerfer G, Bigerelle M, Benayoun S. Wettability versus roughness: multi-scales approach. *Tribol Int.* (2015) **82**(Pt B):343–9. doi: 10.1016/j.triboint.2014.07.002
99. Wissemborski R, Klein R. Welding and marking of plastics with lasers. *Laser Tech J*. (2010) **7**:19–22. doi: 10.1002/latj.201090070
100. Stanford CM. Surface modifications of dental implants. *Aust Dent J*. (2008) **53**:S26–33. doi: 10.1111/j.1834-7819.2008.00038.x
101. Deshpande S, Munoli A. Long-term results of high-density porous polyethylene implants in facial skeletal augmentation: an Indian perspective. *Indian J Plast Surg Off Publ Assoc Plast Surg India* (2010) **43**:34–9. doi: 10.4103/0970-0358.63955
102. Okoshi M, Inoue N. Laser ablation of polymers using 395 nm and 790 nm femtosecond lasers. *Appl Phys Mater Sci Process*. (2004) **79**:841–4. doi: 10.1007/s00339-004-2815-7
103. Ahad IU, Budner B, Korczyc B, Fiedorowicz H, Bartnik A, Kostecki J, et al. Polycarbonate polymer surface modification by extreme ultraviolet (EUV) radiation. *Acta Phys Pol A* (2014) **125**:924–8. doi: 10.12693/APhysPolA.125.924
104. Ahad IU, Butruk B, Ayele M, Budner B, Bartnik A, Fiedorowicz H, et al. Extreme ultraviolet (EUV) surface modification of polytetrafluoroethylene (PTFE) for control of biocompatibility. *Nucl Instrum Methods Phys Res Sect B Beam Interact Mater Atoms* (2015) **364**:98–107. doi: 10.1016/j.nimb.2015.08.093
105. Günther D, Scharnweber D, Hess R, Wolf-Brandstetter C, Grosse Holthaus M, Lasagni AF. High precision patterning of biomaterials using the direct laser interference patterning technology. In: Vilar R, editor. *Laser Surface Modification of Biomaterials*. Cambridge, MA: Woodhead Publishing (2016). doi: 10.1016/B978-0-08-100883-6.00001-0
106. Deepak KLN, Kuladeep R, Kumar VP, Rao SV, Rao DN. Spectroscopic investigations of femtosecond laser irradiated polystyrene and fabrication of microstructures. *Opt Commun*. (2011a) **284**:3074–8. doi: 10.1016/j.optcom.2011.02.001
107. Deepak KLN, Kuladeep R, Venugopal Rao S, Narayana Rao D. Luminescent microstructures in bulk and thin films of PMMA, PDMS, PVA, and PS fabricated using femtosecond direct writing technique. *Chem Phys Lett*. (2011b) **503**:57–60. doi: 10.1016/j.cplett.2010.12.069
108. Pavithra D, Doble M. Biofilm formation, bacterial adhesion and host response on polymeric implants - Issues and prevention. *Biomed Mater*. (2008) **3**:1–13. doi: 10.1088/1748-6041/3/3/034003
109. Wassmann T, Kreis S, Behr M, Wassmann T, Kreis S, Buergers R, et al. The influence of surface texture and wettability on initial bacterial adhesion on titanium and zirconium oxide dental implants. *Int J Implant Dent*. (2017) **3**:32. doi: 10.1186/s40729-017-0093-3
110. Chebolu A, Laha B, Ghosh M. Nagahanumaiah Investigation on bacterial adhesion and colonisation resistance over laser-machined micro patterned surfaces. *IET Micro Nano Lett*. (2013) **8**:280–3. doi: 10.1049/mnl.2013.0109
111. Cunha A, Elie AM, Plawinski L, Serro AP, Botelho do Rego AM, Almeida A, et al. Femtosecond laser surface texturing of titanium as a method to reduce the adhesion of *Staphylococcus aureus* and biofilm formation. *Appl Surf Sci*. (2016) **360**(Pt B):485–93. doi: 10.1016/j.apsusc.2015.10.102
112. Rosenkranz A, Hans M, Gachot C, Thome A, Bonk S, Mücklich F. Direct laser interference patterning: tailoring of contact area for frictional and antibacterial properties. *Lubricants* (2016) **4**:2. doi: 10.3390/lubricants4010002
113. Dalby MJ, Gadegaard N, Tare R, Andar A, Riehle MO, Herzyk P, et al. The control of human mesenchymal cell differentiation using nanoscale symmetry and disorder. *Nat Mater*. (2007) **6**:997. doi: 10.1038/nmat2013
114. Olivares-Navarrete R, Hyzy SL, Hutton DL, Erdman CP, Wieland M, Boyan BD, et al. Direct and indirect effects of microstructured titanium substrates on the induction of mesenchymal stem cell differentiation towards the osteoblast lineage. *Biomaterials* (2010) **31**:2728–35. doi: 10.1016/j.biomaterials.2009.12.029
115. Gittens RA, Olivares-Navarrete R, Cheng A, Anderson DM, McLachlan T, Stephan I, et al. The roles of titanium surface micro/nanotopography and wettability on the differential response of human osteoblast lineage cells. *Acta Biomater*. (2013) **9**:6268–77. doi: 10.1016/j.actbio.2012.12.002
116. Tillotson M, Logan N, Brett P. Osteogenic stem cell selection for repair and regeneration. *Bone Rep*. (2016) **5**:22–32. doi: 10.1016/j.bonr.2016.01.003
117. Conde JC, Riveiro A, Comesana R, Pou J. Theoretical and experimental approach to the texturization process of bioreactive surfaces by high-power laser. *Appl Phys A* (2011) **105**:479–86. doi: 10.1007/s00339-011-6586-7


**Conflict of Interest Statement:** The authors declare that the research was conducted in the absence of any commercial or financial relationships that could be construed as a potential conflict of interest.